



Cite this: *Chem. Commun.*, 2015, 51, 711

Received 12th October 2014,
Accepted 7th November 2014

DOI: 10.1039/c4cc08069f

www.rsc.org/chemcomm

Multiple and configurable optical logic systems based on layered double hydroxides and chromophore assemblies†

Wenyng Shi, Yi Fu, Zhixiong Li and Min Wei*

Multiple and configurable fluorescence logic gates were fabricated via self-assembly of layered double hydroxides and various chromophores. These logic gates were operated by observation of different emissions with the same excitation wavelength, which achieve YES, NOT, AND, INH and INHIBIT logic operations, respectively.

Molecular systems capable of information processing, which are potentially used to develop molecular scale electronics, chemical and biological computers, have received a great deal of attention.¹ Since the proposal of the first molecular AND logic gate by de Silva and co-workers in 1993,² a variety of Boolean logic gates (AND, OR and NOT gate, *etc.*) based on unimolecular systems have been developed.³ However, even with multiple inputs, unimolecular logic gates allow only basic logic operations on single bits of information.⁴ In order to simulate the components and devices with multibyte information processing, it is necessary to construct multimolecular logic gates. In this regard, supramolecular systems can exhibit complex physicochemical properties and perform nontrivial functionalities, which is especially suited for the construction of multicomponent systems. Therefore, the key issue in the design of multimolecular logic gates lies on how individual molecules integrated within a supramolecular platform can transfer signals from one to the other.⁵

Recently, organic fluorescence molecule-based logic systems have attracted remarkable interest owing to their high sensitivity and detectable fluorescence signals at the single molecule level.⁶ In addition, the property of fluorescence resonance energy transfer (FRET), in which excited energy is transferred from a donor to an acceptor chromophore,⁷ provides a promising approach for the connecting logic operations implemented on different molecules. However, organic chromophores generally suffer from instability, bleaching and quenching, which ultimately leads to declined logic capability.

Therefore, how to obtain stable or even enhanced signal of organic chromophore-based logic gates remains a considerable challenge. Recently, inorganic nanosheets of layered double hydroxides (LDHs)⁸ have been utilized to immobilize organic fluorescence anions,⁹ and the resulting composites show significant enhancement in terms of their stability, fluorescence intensity and efficiency.¹⁰ Therefore, this inspires us to challenge the construction of multimolecular logic gates based on the assembly of LDH nanosheets and various fluorescence molecules. It is critical to employ matchable fluorescent molecules and to enrich assembly methods for the combination of chromophores and LDH nanosheets, so as to construct multiple and configurable fluorescence logic gates with high stability and excellent efficiency of signal transmission.

In this work, three fluorescent molecules containing sulfonated poly(*p*-phenylene) (APPP, Fig. 1a), fluorescein (FLU, Fig. 1b) and ethidium bromide (EB, Fig. 1c) were used as model chromophores to incorporate with LDH nanosheets due to their dual FRET property (Fig. S1, ESI†). The resulting multiple logic gate contains

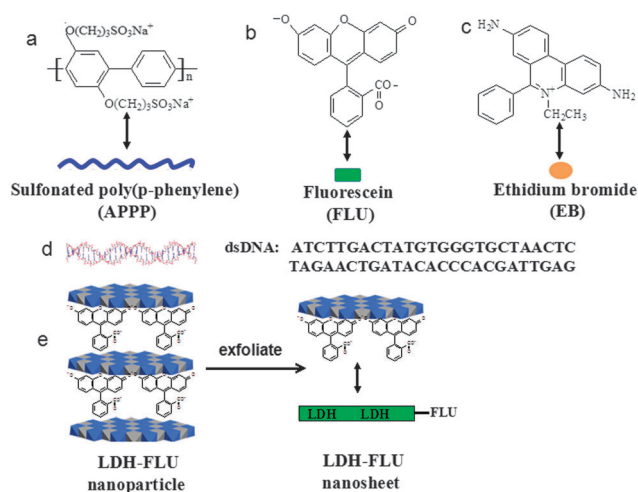


Fig. 1 Chemical structures of (a) APPP, (b) FLU, (c) EB, (d) nucleotide sequences dsDNA, (e) the schematic representation of an LDH-FLU nanoparticle and a single nanosheet.

State Key Laboratory of Chemical Resource Engineering, Beijing University of Chemical Technology, Beijing 100029, P. R. China.

E-mail: weimin@mail.buct.edu.cn; Fax: +86-10-64425385; Tel: +86-10-64412131

† Electronic supplementary information (ESI) available: Preparation and performance of these UTFs, the logic gate operation and their stability. See DOI: 10.1039/c4cc08069f

triple compositions: (1) the conjugated polymer APPP was chosen as the light-harvesting unit owing to its strong light absorption, a large molar extinction coefficient and high quantum yield,¹¹ which can be assembled directly with LDH nanosheets thanks to its abundant negative charge (Fig. S2, ESI[†]); (2) for the assembly of FLU with LDH nanosheets, intercalation of FLU into the interlayer region of LDH nanoparticles followed by exfoliation was carried out, owing to the insufficient negative charge of FLU molecules (Fig. 1e and Fig. S3, ESI[†]); and (3) in the case of the EB cation, DNA (Fig. 1d) was applied both as the building unit for the assembly with LDH nanosheets and as the support for the intercalation of EB into its cavity¹² (Fig. S4A, ESI[†]). By combining the assembly methods mentioned above, a multiple and configurable system of (APPP/LDH-FLU/DNA-EB)_n ultrathin films (UTFs) was obtained (Fig. S4B, ESI[†]), in which a dual FRET occurs *via* a two-step sequence: energy transfer from APPP to FLU, followed by a further transfer from FLU to EB. The different fluorescence emissions of APPP (blue), FLU (green) and EB (yellow) provide the chance to integrate multiple logic operations in parallel. Therefore, the corresponding logic gates (YES, NOT, AND, INH and INHIBIT) were designed by controlling the energy transfer process among APPP, FLU and EB components.

The (APPP/LDH-FLU/DNA)_n UTFs were fabricated by a layer-by-layer assembly method through alternate deposition of APPP, LDH-FLU and DNA on quartz substrates for *n* cycles. In order to obtain highly efficient FRET in the process of logic operation, the optical characterization of the UTFs was investigated. Fig. S5A (ESI[†]) shows the UV-vis absorption spectra of the (APPP/LDH-FLU/DNA)_n UTFs with various trilayer numbers (*n*). It is observed that the absorption bands of DNA, APPP and FLU at ~260, 350 and 501 nm (π - π^* transition) correlate linearly with *n*, respectively (inset in Fig. S5A, ESI[†]), indicating a stepwise and regular film growth procedure. SEM (Fig. S6A, ESI[†]) was further performed to monitor the deposition process of the (APPP/LDH-FLU/DNA)_n UTFs, from which an approximately linear increase of the film thickness (25–126 nm) as a function of the trilayer number (*n* = 5–25) is observed (Fig. S6B, ESI[†]), indicating a uniform and periodic layered structure. Fig. S5B (ESI[†]) reveals that the fluorescence emission intensity of the (APPP/LDH-FLU/DNA)_n UTFs at 435 and 525 nm attributed to APPP and FLU, respectively, increases gradually along with *n* from 5 to 25. The largest value of fluorescence intensity ratio (I_{525}/I_{435}) is located at *n* = 20 (inset in Fig. S5B, ESI[†]), demonstrating the optimum FRET between APPP and FLU. Therefore, *n* = 20 was chosen for further study in the next section.

The YES gate, a single-input gate, is the simplest logic device and the NOT logic corresponds to an inversion of the YES logic.¹³ The YES and NOT gates were realized based on the (APPP/LDH-FLU/DNA)₂₀ UTF by combining an APPP polymer, an LDH-FLU nanosheet and a DNA molecule (Fig. 2A). The YES and NOT logic gate was manipulated by immersing the UTF into EB solution, in which EB as the input (I) can be intercalated into the cavity of DNA. The fluorescence emissions of the (APPP/LDH-FLU/DNA)₂₀ UTF at 525 nm (O₁, the maximum emission of FLU) and 600 nm (O₂, the maximum emission of EB) were used as outputs. The excitation wavelength was 350 nm, which is the maximum absorption of APPP.¹⁴ Fig. 2B shows the fluorescence emission spectra of the (APPP/LDH-FLU/DNA)₂₀ UTF in the presence and absence of EB, and their relation to integrated YES

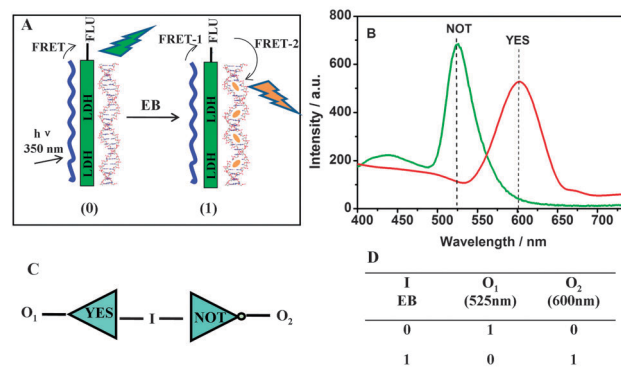


Fig. 2 (A) A schematic representation of the molecular basis of YES and NOT logic operations. (B) Fluorescence emission spectra of the (APPP/LDH-FLU/DNA)₂₀ UTF (green line) and the (APPP/LDH-FLU/DNA-EB)₂₀ UTF (red line) (excitation wavelength λ_{ex} = 350 nm, [EB] = 10^{-3} M). (C) The combinatorial logic scheme. (D) The truth table of the YES and NOT logic gate.

and NOT logic in parallel. The fluorescence intensity at 525 nm is high (1) without EB and low (0) when EB is incorporated into the UTF; while the fluorescence intensity at 600 nm is high (1) in the presence of EB and low (0) in the absence of EB. Therefore, correlating the presence or absence of EB with the emission intensity at 525 nm and 600 nm provides a NOT and a YES logic, respectively. A schematic representation and the truth table of the logic gates are shown in Fig. 2C and D, respectively.

The INH function can be interpreted as a particular integration of AND and NOT logic functions, where the output signal is inhibited by the input.¹⁵ In this case, an INH gate can be created based on the (LDH-FLU/DNA)₂₀ UTF, which was manipulated by utilizing APPP (I₁) and EB (I₂) as the inputs while the emission at 525 nm (O₁) was used as the output. Fig. 3 shows the four possible input combinations ((0,0), (0,1), (1,0), (1,1)) for an INH gate. A strong signal of FLU emission at 525 nm is observed only in the presence of APPP and in the absence of EB. At the same time, when monitoring at 600 nm (O₂), the (1,1) combination shows a strong fluorescence intensity, which corresponds to the AND logic. Therefore, the integrated INH and AND logic operation in parallel is also obtained.

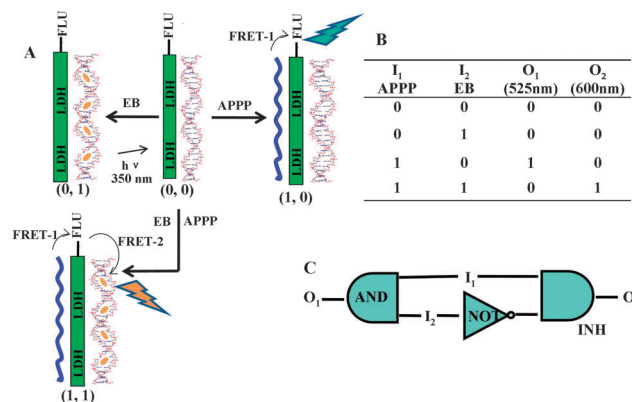


Fig. 3 (A) A schematic representation of the molecular basis of AND and INH logic operation. (B) The truth table of the AND and INH gate. (C) The combinatorial logic scheme.

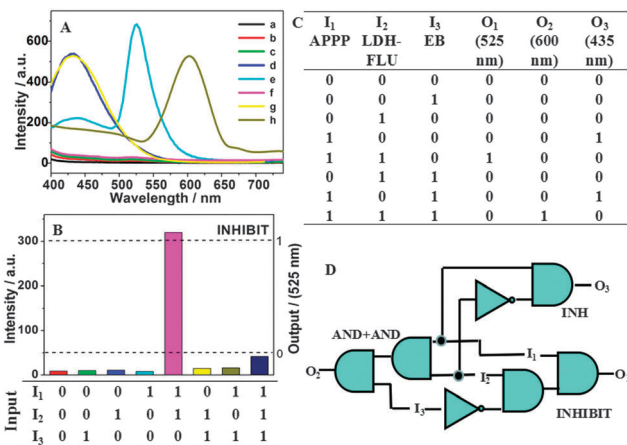


Fig. 4 (A) A schematic representation of the molecular basis of AND + AND, INH, and INHIBIT logic operation: (a) the (LDH/DNA)₂₀ UTF, (b) the (LDH/DNA-EB)₂₀ UTF, (c) the (LDH-FLU/DNA)₂₀ UTF, (d) the (APPP/LDH/DNA)₂₀ UTF, (e) the (APPP/LDH-FLU/DNA)₂₀ UTF, (f) the (LDH-FLU/DNA-EB)₂₀ UTF, (g) the (APPP/LDH/DNA-EB)₂₀ UTF, (h) the (APPP/LDH-FLU/DNA-EB)₂₀ UTF. (B) The fluorescence intensity of the INHIBIT gate at 525 nm from the eight possible input combinations ($\lambda_{\text{ex}} = 350$ nm, [EB] = 10^{-3} M). (C) The truth table of the AND + AND, INH and INHIBIT gate. (D) The combinatorial logic scheme.

By combining the molecular components of AND and NAND gates, a three-input INHIBIT logic gate can be constructed with the (LDH/DNA)₂₀ UTF. The inputs for the INHIBIT gate are APPP (I_1), FLU (I_2) and EB (I_3); while the emission at 525 nm (irradiation at 350 nm) is used as the output (Fig. 4A and Fig. S7, ESI[†]). The third input (EB) inhibits the output of the logic gate. In the absence of EB, a strong fluorescence signal at 525 nm was observed for the INHIBIT gate in the presence of I_1 and I_2 (Fig. 4B). A more complicated logic can be implemented, which is provided by the three emissions in the (APPP/LDH-FLU/DNA-EB)₂₀ assembly. Upon monitoring at 600 nm (O_2), a strong emission is present only for the (1,1,1) combination, conforming to the integrated logic of two AND gates. In the presence of APPP and the absence of FLU, a strong signal of APPP emission at 435 nm (O_3) is observed whether EB is present or not. This combination thus corresponds to the INH logic (Fig. 4C and D).

The stability of a logic gate operation is absolutely critical, which may result in declined, wrong readout and even the breakdown of logic ability in extreme cases. Fig. S8 (ESI[†]) shows the fluorescence intensity of the (APPP/LDH/DNA)₂₀ UTF, the (LDH-FLU/DNA)₂₀ UTF, the (LDH/DNA-EB)₂₀ UTF, pristine APPP, FLU and EB in aqueous solution upon irradiation with UV light for a comparison study. It is observed that the half-life of the UTF samples (5 min for the (APPP/LDH/DNA)₂₀ UTF, 5 h for the (LDH-FLU/DNA)₂₀ UTF and 1 h for the (LDH/DNA-EB)₂₀ UTF) is much longer than the corresponding aqueous solutions (2 min for APPP, 2 h for FLU and 40 min for EB). Moreover, ~94% of the initial fluorescence intensity was maintained even after one month measurement of the UTF samples (Fig. S9, ESI[†]). Therefore, the results show that the photo- and storage stability of APPP, FLU and EB molecules are significantly enhanced in the LDH matrix. In addition, these UTFs show good reproducibility with RSD $\leq 3.0\%$ for 5 independent measurements (Fig. S10, ESI[†]).

In summary, YES, NOT, AND, INH and INHIBIT logic gate functions with fluorescence readout were successfully achieved by employing various assembly methods (electrostatic interaction, intercalation-exfoliation and intercalation) based on three chromophore components. The simultaneous integration of multiple logic operations in parallel was carried out based on fluorescence emissions of APPP, FLU and EB, by monitoring different emissions (435, 525 and 600 nm) with the same excitation wavelength (350 nm). In addition, these chemical logic devices display largely enhanced photo- and storage stability as well as good reproducibility. This strategy can be further expanded to the development of other molecular logic gates with fluorescence readout by virtue of the variety of organic chromophores and versatility in assembly methods. It is expected that these logic gates can be potentially applied in the detection and measurement of multi-analyte or real-time information of complicated samples in analytical chemistry and environmental science.

This work was supported by the 973 Program (Grant No. 2014CB932104), the National Natural Science Foundation of China, the Scientific Fund from Beijing Municipal Commission of Education (20111001002), the Fundamental Research Funds for the Central Universities (ZD 1303 and ZY1325) and the Scientific Research Foundation for the Overseas Chinese Scholars.

Notes and references

- (a) E. Katz and V. Bocharova, in *Molecular and supramolecular information processing*, ed. E. Katz, Wiley-VCH, 2012, p. 1; (b) D. Gust, J. Andréasson, U. Pischel, T. A. Moore and A. L. Moore, *Chem. Commun.*, 2012, **48**, 1947; (c) K. Szacitowski, *Chem. Rev.*, 2008, **108**, 3481; (d) J. Zhou, J. Halánek, V. Bocharova, J. Wang and E. Katz, *Talanta*, 2011, **83**, 955; (e) E. Katz, J. Wang, M. Privman and J. Halánek, *Anal. Chem.*, 2012, **84**, 5463; (f) M. Chuang, J. R. Windmiller, P. Santhosh, G. V. Ramirez, E. Katz and J. Wang, *Chem. Commun.*, 2011, **47**, 3087; (g) J. Wang and E. Katz, *Isr. J. Chem.*, 2011, **51**, 141.
- A. P. de Silva, H. Q. N. Gunaratne and C. P. McCoy, *Nature*, 1993, **364**, 42.
- (a) H. Tian, *Angew. Chem., Int. Ed.*, 2010, **49**, 4710; (b) J. Cao, X. Ma, M. Min, T. Cao, S. Wu and H. Tian, *Chem. Commun.*, 2014, **50**, 3224.
- J. Andréasson, U. Pischel, S. D. Straight, T. A. Moore, A. L. Moore and D. Gust, *J. Am. Chem. Soc.*, 2011, **133**, 11641.
- V. Balzani, A. Credi and M. Venturi, *ChemPhysChem*, 2003, **3**, 49.
- (a) Z. Q. Guo, W. H. Zhu and H. Tian, *Chem. Commun.*, 2012, **48**, 6073; (b) J. Andréasson and U. Pischel, *Chem. Soc. Rev.*, 2010, **39**, 174.
- (a) J. L. Brédas, D. Beljonne, V. Coropceanu and J. Cornil, *Chem. Rev.*, 2004, **104**, 4971; (b) D. Margulies, G. Melman, C. E. Felder, R. Arad-Yellin and A. Shanzer, *J. Am. Chem. Soc.*, 2004, **126**, 15400.
- (a) Q. Wang and D. O'Hare, *Chem. Commun.*, 2013, **49**, 6301; (b) Q. Wang, X. Zhang, J. H. Zhu, Z. H. Guo and D. O'Hare, *Chem. Commun.*, 2012, **48**, 7450; (c) D. P. Yan, J. Lu, M. Wei, J. Ma, D. G. Evans and X. Duan, *Chem. Commun.*, 2009, 6358.
- D. P. Yan, J. Lu, M. Wei, S. H. Qin, L. Chen, S. T. Zhang, D. G. Evans and X. Duan, *Adv. Funct. Mater.*, 2011, **21**, 2497.
- (a) Q. Wang and D. O'Hare, *Chem. Rev.*, 2012, **112**, 4124; (b) D. P. Yan, J. Lu, L. Chen, S. Qin, J. Ma, M. Wei, D. G. Evans and X. Duan, *Chem. Commun.*, 2010, **46**, 5912.
- (a) A. Okamoto, K. Tanaka and I. Saito, *J. Am. Chem. Soc.*, 2004, **126**, 9458; (b) J. H. Reif, *Science*, 2002, **296**, 478.
- Y. N. Teo and E. T. Kool, *Chem. Rev.*, 2012, **112**, 4221.
- A. P. de Silva, N. D. McClenaghan and C. P. McCoy, in *Molecular Switches*, ed. B. L. Feringa, Wiley-VCH, 2001, p. 339.
- D. P. Yan, J. Lu, M. Wei, J. B. Han, J. Ma, F. Li, D. G. Evans and X. Duan, *Angew. Chem., Int. Ed.*, 2009, **48**, 3073.
- V. Balzani, A. Credi and M. Venturi, in *Molecular Devices and Machines. A Journey Into the Nanoworld*, ed. V. Balzani, M. Venturi and A. Credi, Wiley-VCH, 2003, p. 235.